Mon. Not. R. Astron. Soc. **000**, 000–000 (0000) Printed 2 February 2008 (MN LaTeX style file v2.2)

# The Correlation Between Spectral Index And Accretion Rate For AGN

Xue-Guang Zhang[1,3⋆], Deborah Dultzin[1], Ting-Gui Wang[2]
[1] *Instituto de Astronomía, Universidad Nacional Autónoma de México, Apdo Postal 70-264, México D. F. 04510, Mexico*
[2] *Center for Astrophysics, Department of astronomy and Applied Physics, University of Science and Technology of China, Hefei, Anhui, P.R.China*
[3] *Max-Plank Institute für Astrophysik, Karl-Schwarzschild-str 1, 85748 Garching, Germany*



**ABSTRACT**
In this paper, we present a correlation between the spectral index distribution (SED) and the dimensionless accretion rate defined as $\dot{m} = L_{bol}/L_{Edd}$ for AGN. This quantity is used as a substitute of the physical accretion rate. We select 193 AGN with both broad H$\alpha$ and broad H$\beta$, and with absorption lines near MgI$\lambda$5175$\mathring{A}$ from SDSS DR4. We determine the spectral index and dimensionless accretion rate after correcting for both host galaxy contribution and internal reddening effects. A correlation is found between the optical spectral index and the dimensionless accretion rate for AGN, including low luminosity AGN ($L_{H\alpha} < 10^{41}\mathrm{erg\cdot s^{-1}}$ sometimes called "dwarf AGN" (Ho et al. 1997)). The existence of this correlation provides an independent method to estimate the central BH masses for all types of AGN. We also find that there is a different correlation between the spectral index and the BH masses for normal AGN and low luminosity AGN, which is perhaps due to the different accretion modes in these two types of nuclei. This in turn may lead to the different correlations between BH masses and optical continuum luminosity reported previously (Zhang et al. 2007a), which invalidates the application of the empirical relationship found by Kaspi et al. (2000, 2005) to low luminosity AGN in order to determine their BLR sizes.

**Key words:** Galaxies:Active – Galaxies:nuclei – Galaxies:emission lines

## 1 INTRODUCTION

Because of the difficulty to calculate the physical accretion rate to the BH in an AGN, a dimensionless accretion rate can be defined and estimated based on the bolometric luminosity and BH mass, $\dot{m} = \frac{L_{bol}}{L_{Edd}}$. This parameter can be used as the substitute for the actual accretion rate. Moreover, the dimensionless accretion rate is an important parameter in the scheme of the so called unified model for AGN (Antonucci 1993, Quintilio & Viegas 1997, Urry & Padovani 1995), and also the 4D Eigenvector 1 Scheme (e.g., Dultzin-Hacyan et al. (2007). The difference in accretion rate leads to the principal difference between high luminosity QSOs and low luminosity Seyfert galaxies. It seems to be also one of the main physical parameters underlying the 4D Eigenvector 1 Scheme as explained recently in Dultzin-Hacyan et al. (2007). In order to obtain the dimensionless accretion rate $\dot{m}$, two other parameters must be calculated first: BH mass $M_{BH}$ and the bolometric luminosity $L_{bol}$.

The common method to estimate the bolometric luminosity $L_{bol}$ of AGN is based on the continuum luminosity from the nuclei: $L_{bol} \sim 9 \times L_{5100\mathring{A}}$ given by Kaspi et al. (2000) and confirmed by Shang et al. (2005) for QSOs. Recently, the relation was used by Bonning et al. (2007) to study the correlation between the accretion disk temperatures and the continuum colors in QSOs. However, it should be stressed that the relation does not hold for ALL kinds of AGN, in particular, for low luminosity AGN (Ho et al. 1997a, 1997b, Ho 1999), because of the different Spectral Energy Distribution (SED) (the lack of the Big Blue Bump).

Several methods are used to estimate BH masses of AGN. The most reliable method is based on the stellar velocity dispersion of the bulge of the host galaxy first presented by Ferrarese & Merritt (2000) and Gebhardt et al. (2000), then confirmed by Tremaine et al. (2002) and Merritt & Ferrarese (2001) etc.

$$M_{BH} = 10^{8.13\pm0.06}(\frac{\sigma}{200\mathrm{km\cdot s^{-1}}})^{4.02\pm0.32}\mathrm{M_\odot} \qquad (1)$$

which indicates a strong correlation between BH masses and bulge masses (Häing & Rix 2004, Marconi & Hunt 2003, McLure & Dunlop 2002, Laor 2001, Kormendy 2001, Wandel 1999) etc. However we should note that the relation of $M_{BH} - \sigma$ is obtained through the results of nearby inactive galaxies. Whether the relation can be applied to far away

⋆ xueguang@mpa-garching.mpg.de

active galaxies is an interesting question. So far, there are a few dynamical mass estimates of central black holes of broad line AGN, and the BH masses are consistent with the BH masses estimated from the relation of $M_{BH} - \sigma$, although the uncertainties are still large. In addition, we should say that the objects in our sample described in the following section are not high luminosity and high redshift QSOs, thus the correlation between central black hole and bulge of host galaxy can be reasonably considered to hold.

The other methods are based on the assumption of virialization of the Broad Line Emitting Regions (BLRs), or at least part of them (Peterson et al. 2004, Onken et al. 2004, Sulentic et al. 2006, Dultzin-Hacyan et al. 2007). In order to calculate the parameter of dimensionless accretion rate, the BH mass is necessary. However, for high luminosity and high redshift AGN, it is difficult to measure the stellar velocity dispersions. The assumption of virialization is applied for QSOs. In order to estimate BH masses of QSOs based on the assumption of virialization, the most convenient way is to use the equation:

$$M_{BH} = f \times \frac{R_{BLRs} \times \sigma_b^2}{G} = 2.15 \times 10^8 (\frac{\sigma_b}{3000\mathrm{km \cdot s^{-1}}})^2 (\frac{L_{5100\mathring{A}}}{10^{44}\mathrm{erg \cdot s^{-1}}})^{0.69} \mathrm{M_\odot} \quad (2)$$

There are, however, some caveats with this method. First, the question of whether the relation $R_{BLRs} \sim L^{0.69}_{5100\mathring{A}}$ found by Kaspi et al. (2000, 2005) can be applied for all AGN, in particular high redshift ones. In an attempt to answer this question, we have found that the relation is not valid for some special kinds of AGN, such as the low luminosity AGN (Zhang, Dultzin-hacyan & Wang 2007a, Wang & Zhang 2003) and the AGN with double-peaked low ionization emission lines (Zhang, Dultzin-Hacyan & Wang 2007b). Second, the estimation of the BH masses of high redshift AGN by means of Equation (2) will lead to BH masses larger than $10^{10}\mathrm{M}\odot$ (meaning $\sigma > 600\mathrm{km \cdot s^{-1}}$), which leads to unreasonable masses of the bulge larger than $10^{13}\mathrm{M}_\odot$ (Netzer 2003, Sulentic et al. 2006). For this reason, finding another parameter which can be observationally determined, related to the dimensionless accretion rate is an important task and is the main objective of this paper. The accretion rate is determined by two properties: the continuum luminosity $L_{5100\mathring{A}}$ and the BH mass $M_{BH}$. The continuum luminosity can be calculated from the observed spectra as discussed in the the next section. Thus, in order to obtain a reliable result, we select Equation (1) to estimate the central BH masses of AGN rather than Equation (2).

The accretion disk model has been widely accepted as the standard model for AGN. In the NLTE (Non Local Thermodynamic Equilibrium) accretion disk mode, the generated SED (Spectral Energy Distribution) is based on three main parameters: BH masses $M_{BH}$, accretion rate $\dot{M}$ and the viscosity parameter $\alpha$. An expected result is that there should be a correlation between the spectral index and the accretion rate $\dot{m}$. In this paper, we answer the question whether the observed spectral index can be used to trace the dimensionless accretion rate. In section II, we present the data sample. Section III gives the results. Finally the discussion and conclusions are given in Section IV. In this paper, the cosmological parameters $H_0 = 70\mathrm{km \cdot s^{-1}Mpc^{-1}}$, $\Omega_\Lambda = 0.7$ and $\Omega_m = 0.3$ have been adopted.

## 2 DATA SAMPLE

We select objects from SDSS DR4 (Adelman-McCarthy et al. 2006) to make up our sample according to the following two criteria: First, and most important is that the objects' spectra present absorption features, here we focused on the absorption line MgI$\lambda 5175\mathring{A}$, in order to measure the stellar velocity dispersion of the bulge. Second, in order to obtain the intrinsic continuum luminosity from the nuclei after the correction of internal reddening effects using the Balmer decrement, Balmer emission lines, both H$\alpha$ and H$\beta$ must be also present. In order to perform accurate measurements of the lines mentioned above, several procedures have to be followed.

In order to obtain the continuum luminosity from the nuclei we must subtract first the contribution of stellar light. An efficient method to subtract the stellar light is the PCA (Principle Component analysis) method described by Li et al. (2005) and Hao et al. (2005), using the eigenspectra from pure absorption galaxies from SDSS or the eigenspectra from stars in STELIB (Le Borgne et al. 2003), because the method of Principle Component Analysis (PCA) provides a better way to constrict more favorable information from a series of spectra of stars or galaxies into several eigenspectra. Here, we used the method from Hao et al. (2005). The eigenspectra are calculated by KL (Karhunen-Loeve) transformation for about 1500 pure absorption galaxies selected from SDSS DR4. Then, the first eight eigenspectra and the spectra of an A star (which is used to account for star formation) selected from STELIB (Le Borgne et al. 2003) are used to fit the stellar properties of the observed spectra. After this, rather than a power law, a three-order polynomial function is used to fit the featureless continuum, because the study of composite spectra of AGN shows that the continuum should be best fitted by two power laws with a break of $\sim 5000\mathring{A}$ (Francis et al. 1991, Zheng et al. 1997, Vanden Berk et al. 2001). After the last step, the featureless continuum and the stellar components are obtained based on the Levenberg-Marquardt least-squares minimization method.

After the subtraction of stellar components and the continuum emission, the line parameters of emission lines can be measured by Levenberg-Marquardt least-squares minimization: one gaussian function for each forbidden emission line, two gaussian functions (one broad and one narrow) for each permitted emission line. For [OIII]$\lambda 4959, 5007\mathring{A}$, we use an extra gaussian function for the extended wings as shown in Greene & Ho (2005a). Then we select the objects with reliable broad H$\alpha$ and broad H$\beta$ according to the following criteria: $\sigma(B) \geqslant 3 \times \sigma(B)_{err}$, $flux(B) \geqslant 3 \times flux(B)_{err}$ and $\sigma(B) \geqslant 600\mathrm{km \cdot s^{-1}}$, where 'B' represents the values for the broad Balmer components, 'err' means the measured error of the value, $\sigma$ is the second moment of broad Balmer emission lines.

Then it is necessary to measure the stellar velocity dispersions of the objects selected. However, the accurate measurement of stellar velocity dispersion is an open question, because of the known problems with the template mismatch. A commonly used method is to select spectra of several

kinds of stars (commonly, G and K) as templates, and then broaden the templates by the same velocity to fit stellar features, leaving the contributions from different kinds of stars as free parameters (Rix & White 1992). However, more information about stars included by the templates should lead to more accurate measurement of stellar velocity dispersion. According to the above mentioned method to subtract stellar components, we created a new template rather than several spectra of G or K stars as templates. Thus, we apply the PCA method for all 255 spectra of different kinds of stars in STELIB. Selecting the first several eigenspectra and a three-order polynomial function for the background as templates, the value of stellar velocity dispersion can be measured by the minimum $\chi^2$ method applied to the absorption features around MgI$\lambda$5175$\mathring{A}$ within the wavelength range from 5100$\mathring{A}$ to 5300$\mathring{A}$ (Zhang, Dultzin-Hacyan & Wang 2007c). Finally, we select the objects for which the measured values of stellar velocity dispersions are at least three times larger than the measured errors.

Finally, we select 193 AGN with redshift from 0.015 to 0.25 and with observed featureless continuum luminosity within the range from $10^{41.23}\mathrm{erg\cdot s^{-1}}$ to $10^{43.79}\mathrm{erg\cdot s^{-1}}$ from about 400000 objects classified as galaxies in SDSS DR4. The objects have reliable stellar velocity dispersions and reliable broad Balmer emission lines.

## 3 RESULTS FROM THE DATABASE OF SDSS

Before proceeding further, a simple discussion about the origin of the featureless continuum emission is given. Basically, the possibility of nebular emission can be rejected. According to the luminosity of Recombination lines, the nebular continuum emission at 5100$\mathring{A}$ can be simply estimated by $L_{5100\mathring{A},Nebulae} \sim 0.1 \times L_{H\beta}$, if the electron temperature $T = 10^4$K is accepted. Thus the effects of nebular emission can be neglected. Furthermore, we check the correlation between continuum luminosity and the luminosity of Balmer emission lines found by Greene & Ho (2005b). The result is shown in Figure 1. We should note that the continuum luminosity and luminosity of H$\alpha$ are the values before the internal reddening correction as shown in Greene & Ho (2005b). The coincident correlation between $L_{5100\mathring{A}}$ and $L_{H\alpha}$ ( including the narrow component) indicates that our method to subtract the stellar components is reliable to some extent. Based on the correlation of $L_{H\alpha} - L^{1.157}_{5100\mathring{A}}$ for AGN with high continuum luminosity, we can estimate the effects of star formation on the continuum luminosity. For AGN with low luminosity and low redshift, there are two components in narrow H$\alpha$, one from the AGN $L_{H\alpha,AGN}$ and the other one from star formation $L_{H\alpha,SF}$ (Kauffmann et al. 2003). Moreover, we assumed the continuum luminosity also includes two components, one from the AGN $L_{5100\mathring{A},AGN}$ and the other one from star formation $L_{5100\mathring{A},SF}$. Furthermore, there is a strong correlation between line and continuum luminmosities shown in Figure 1, $L_{H\alpha,SF}+L_{H\alpha,AGN} \propto (L_{5100\mathring{A},SF}+L_{5100\mathring{A},AGN})^{1.157}$. We can simply estimate the effects of star formation on continuum luminosity, if we accept that $L_{H\alpha,SF} = s \times L_{H\alpha,AGN}$ and $L_{H\alpha,AGN} \propto L^{1.157}_{5100\mathring{A},AGN}$ (because the relation is better applied for high luminosity AGN with less effects of star formation):

$$\begin{aligned} &L_{H\alpha,SF} + L_{H\alpha,AGN} \sim (L_{5100\mathring{A},SF} + L_{5100\mathring{A},AGN})^{1.157} \\ &L_{H\alpha,AGN} \sim L^{1.157}_{5100\mathring{A},AGN} \\ &1 + s \sim (1 + \frac{L_{5100\mathring{A},SF}}{L_{5100\mathring{A},AGN}})^{1.157} \end{aligned} \quad (3)$$

If we accepted that star-forming regions contribute 65% of the narrow H$\alpha$ flux as described in Kauffmann et al. (2003), the parameter of $s$ can be determined as:

$$\begin{aligned} s &= \frac{L_{H\alpha,SF}}{L_{H\alpha,AGN}} \\ &= \frac{0.65 \times L_{H\alpha,N}}{L_{H\alpha,B} + 0.35 \times H_{H\alpha,N}} \end{aligned} \quad (4)$$

where 'N' and 'B' represent the narrow component and broad component of H$\alpha$. The mean value of $L_{H\alpha,B}/L_{H\alpha,N}$ is about 3.96 for the objects in our sample. Then we can determine that $L_{5100\mathring{A},SF}/L_{5100\mathring{A},AGN} \sim 0.12$, i.e., the star-forming regions contribute about 10% of the observed continuum luminosity. Thus in the following section, we can ignore the effects of star fromation.

In order to obtain a reliable intrinsic continuum shape, the internal reddening effects must be corrected. The common way to correct them is through the Balmer decrement. Here, we assume the intrinsic Balmer decrement as 3.1 for H$\alpha$ and H$\beta$ expected by Case B recombination (albeit it is debatable wether it can be applied to broad lines) with some contributions from collisional excitation. Then, the value of E(B-V) can be determined from the Balmer decrement:

$$\mathrm{E(B-V)} = -0.97615448 + 1.9866313 \log(\frac{\mathrm{H}\alpha}{\mathrm{H}\beta}) \quad (5)$$

where $\frac{\mathrm{H}\alpha}{\mathrm{H}\beta}$ is the observed flux ratio. This equation calculated from the R-dependent Galactic extinction curve presented by Fitzpatrick (1999) can be used to calculate the value of E(B-V) simply through the Balmer decrement. In the following of the paper, the continuum luminosity and luminosity of H$\alpha$ are the ones after the correction of BLRs extinction.

After the correction of internal reddening effects, the spectral index can be determined. Here we select three spectral indices: $\frac{F_{4400\mathring{A}}}{F_{5100\mathring{A}}}$, $\frac{F_{5100\mathring{A}}}{F_{6800\mathring{A}}}$ and $\frac{F_{4400\mathring{A}}}{F_{6800\mathring{A}}}$. The BH masses are calculated using Equation (1). The internal continuum luminosity after the correction of the internal reddening can also be calculated. Thus it is easy to check the correlation between dimensionless accretion rate and spectral index. Here we should notice that the diminsionless accretion rate for low luminosity AGN as discussed in the introduction and in the next section is also calculated by $\dot{m} = \frac{L_{bol}}{L_{Edd}} \sim \frac{9\times L_{5100\mathring{A}}}{L_{Edd}}$, although, the bolometric luminosity of low luminosity AGN cannot be correctly calculated by $L_{bol} \sim 9\times L_{5100\mathring{A}}$ as shown in Ho (1999). However, to some extent, we can accept that, if there is also a simple relation $L_{bol} \sim k \times L_{5100\mathring{A}}$ for low luminosity AGN, the calculated $\frac{9\times L_{5100\mathring{A}}}{L_{Edd}}$ can be used as a substitute of accretion rate, and it is convenient to compare the properties of low luminosity and normal AGN. The correlations are shown in Figure 2. The Spearman Rank Correlation Coefficient is 0.68 with $P_{null} \sim 1.51\times10^{-27}$, 0.65 with $P_{null} \sim 1.42\times10^{-24}$ and 0.67 with $P_{null} \sim 1.94\times10^{-26}$ for

$\frac{F_{5100\mathring{A}}}{F_{6800\mathring{A}}}$, $\frac{F_{4400\mathring{A}}}{F_{5100\mathring{A}}}$ and $\frac{F_{4400\mathring{A}}}{F_{6800\mathring{A}}}$ respectively. In order to check the effects of internal reddening, we also show the correlation between the dimensionless accretion rate and the spectral index $\frac{F_{5100\mathring{A}}}{F_{6800\mathring{A}}}$ in the right-bottom panel of Figure 2, without internal reddening correction. The Spearman Rank Correlation Coefficient for the correlation without reddening correction is about 0.56 with $P_{null} \sim 2.01 \times 10^{-17}$. The unweighted best fitted results for the correlations between spectral indices and dimensionless accretion rates are shown as solid lines that correspond to:

$$\begin{aligned}
\log(\frac{F_{5100\mathring{A}}}{F_{6800\mathring{A}}}) &= 0.56 + 0.18 \times \log(\frac{9 \times L_{5100\mathring{A}}}{L_{Edd}}) \\
\log(\frac{F_{4400\mathring{A}}}{F_{5100\mathring{A}}}) &= 0.35 + 0.14 \times \log(\frac{9 \times L_{5100\mathring{A}}}{L_{Edd}}) \\
\log(\frac{F_{4400\mathring{A}}}{F_{6800\mathring{A}}}) &= 0.92 + 0.33 \times \log(\frac{9 \times L_{5100\mathring{A}}}{L_{Edd}}) \\
\log(\frac{F_{5100\mathring{A}}}{F_{6800\mathring{A}}})(uncorr) &= 0.37 + 0.14 \times \log(\frac{9 \times L_{5100\mathring{A}}}{L_{Edd}})
\end{aligned} \tag{6}$$

The last expression is for the correlation between spectral index $\frac{F_{5100\mathring{A}}}{F_{6800\mathring{A}}}$ and dimensionless accretion rate without internal reddening correction. Furthermore, we are interested in the absolute scatter in the parameter of spectra index which can be calculated by:

$$\Delta_Y = \sqrt{\frac{\sum_{i=1}^{N}(Y_i - Y_{i,fit})^2}{N}} \tag{7}$$

where $Y_i, Y_{i,fit}$ are the measured value of spectra index and the fitted value by the equations listed in Equation (6). Finally, we can obtain the scatters as follows, $\Delta_{\log(\frac{F5100\mathring{A}}{F6800\mathring{A}})} \sim 0.128$, $\Delta_{\log(\frac{F4400\mathring{A}}{F5100\mathring{A}})} \sim 0.124$, $\Delta_{\log(\frac{F4400\mathring{A}}{F6800\mathring{A}})} \sim 0.227$ and $\Delta_{\log(\frac{F5100\mathring{A}}{F6800\mathring{A}})(uncorr)} \sim 0.123$

We also show the correlation between the line width of broad H$\alpha$ and the line width of broad H$\beta$ in Figure 3. The Spearman Rank Correlation Coefficient is about 0.82 with $P_{null} \sim 0$. The correlation between the line widths of broad Balmer emission lines is:

$$\sigma_{H\beta_B} = (1096.56 \pm 124.74) \times (\frac{\sigma_{H\alpha_B}}{10^3 \mathrm{km \cdot s^{-1}}})^{1.01 \pm 0.02} \mathrm{km \cdot s^{-1}} \tag{8}$$

where $\sigma$ is the measured value using a gaussian function to measure broad emission lines. This correlation is similar to the one for QSOs found by Greene & Ho (2005b), $FWHM_{H\beta} \propto FWHM_{H\alpha}^{1.03 \pm 0.03}$. This indicates that the measurement of line parameters of broad Balmer emission lines is reliable. In addition, it is convenient for us to compare the two kinds of BH masses estimated from Equation (1) and Equation (2). Before proceeding further, we should notice that Equation (2) cannot be applied to the low luminosity AGN discussed in the next section, because of the unreasonable correlation between the size of BLRs and the continuum luminosity found by Kaspi et al. (2000, 2005) (Wang & Zhang 2003, Zhang, Dultzin-Hacyan & Wang 2007a). Thus, here, we select the normal AGN in our sample to estimate the virial BH masses with Equation (2). Finally there are 155 objects shown in Figure 4 to compare the two kinds of BH masses estimated by Equation (1) and Equation (2). The Spearman Rank correlation coefficient is about 0.36 with $P_{null} \sim 4.8 \times 10^{-6}$, after the internal reddening corrections. The correlation also indicates that the measured stellar velocity dispersions, the measured internal continuum luminosities and the line widths are reliable.

## 4 DISCUSSION AND CONCLUSIONS

There are 38 low luminosity AGN with $L_{H\alpha} < 10^{41} \mathrm{erg \cdot s^{-1}}$ (Ho et al. 1997a, 1997b and Ho 1999), which are shown in solid circles in Figure 2. From the figure, we can see that there is no difference in the correlation between spectral index and $\frac{9 \times L_{5100\mathring{A}}}{L_{Edd}}$ for normal AGN and low luminosity AGN. If the bolometric luminosity of low luminosity AGN was different from $9 \times L_{5100\mathring{A}}$, all the low luminosity AGN would deviate from the correlation for normal AGN, due (probably) to different accretion modes. Even if there is a different accretion mode for low luminosity AGN (as suggested by the lack of the big blue bump in the spectra of low luminosity AGN as shown in Ho (1999)), the bolometric luminosity of low luminosity AGN can also be calculated using $L_{bol} \sim k \times L_{5100\mathring{A}}$. Otherwise, we could not find the same correlation between spectral index and $\frac{9 \times L_{5100\mathring{A}}}{L_{Edd}}$ for low luminosity AGN and normal AGN.

According to the accretion disk model, the output SED is the result of the convolution of other parameters as well, such as the central BH mass, the viscosity in the disk, and the inclination angle. However there is no correlation between the spectral index and central BH masses, which is shown in Figure 5. The Spearman Rank Correlation Coefficient is less than 0.1 with $P_{null} > 60\%$ for all objects in our sample. An interesting result is that there is actually a negative trend (anticorrelation) between BH masses and the spectral indexes for the 38 low luminosity AGN. The coefficient is about -0.54 with $P_{null} \sim 4.97 \times 10^{-4}$, -0.52 with $P_{null} \sim 8.62 \times 10^{-4}$ and -0.55 with $P_{null} \sim 3.98 \times 10^{-4}$ for $\frac{F_{5100\mathring{A}}}{F_{6800\mathring{A}}}$, $\frac{F_{4400\mathring{A}}}{F_{5100\mathring{A}}}$ and $\frac{F_{4400\mathring{A}}}{F_{6800\mathring{A}}}$ respectively.

Because of the positive correlation between the spectral index and the accretion rate, a negative correlation between the spectral index and central BH masses could be expected for all AGN. However our results indicate that this expectation is only valid for low luminosity AGN. The reason is probably related to the correlation between BH masses and continuum luminosity. For Normal AGN, there is strong correlation between the BH masses and the continuum luminosity (Peterson et al. 2004). However for low luminosity AGN, this correlation is much weaker (Zhang, Dultzin-Hacyan & Wang 2007a). The correlation between the central BH masses and the internal continuum luminosity is shown in Figure 6. The coefficient is about 0.47 with $P_{null} \sim 9.05 \times 10^{-10}$, however, the coefficient is only 0.12 with $P_{null} \sim 49\%$ for the 38 low luminosity AGN. The same result for low luminosity AGN can be found in Panessa et al. (2006). In their paper, they selected all the low luminosity Seyfert galaxies from Ho, Filippenko & Sargent (1997a, 1997b), and found that there is NO correlation between

the X-ray or optical emission line luminosities (especially [OIII]$\lambda$5007$\mathring{A}$ line) and BH masses. The result also confirms that there is a different accretion mode for normal and low luminosity AGN.

To estimate the effects of the inclination angle of the accretion disk is difficult. However under the assumption that the narrow line emission region is isotropic, we can check the correlation between the continuum luminosity and the luminosity of narrow emission lines. If the objects have very different inclination angles of the accretion disk, a loose correlation between the continuum luminosity and the luminosity of narrow emission line should be expected. Here we show the correlation between $L_{5100\mathring{A}}$ and the luminosity of narrow H$\alpha$ in Figure 7. Although it is more common to use the [OIII]$\lambda$5007$\mathring{A}$ as an isotropic estimator of AGN luminosity, we prefer to use the narrow component of H$\alpha$ because of the following reason. [OIII] emission line frequently cannot be fitted by one single gaussian function, because it has extended wings (Greene & Ho 2005a). The two components are not emitted from the same region. The extended component is probably emitted from the far-side of the BLRs. Thus when we fit the [OIII] line, two gaussian functions are applied as described in Section II. We thus select the narrow component of H$\alpha$ rather than [OIII] to test the effects of inclination angle. A strong correlation can be confirmed. The spearman Rank Correlation Coefficient is about 0.89 with $P_{null} \sim 0$ for normal AGN, and about 0.67 with $P_{null} \sim 4.04 \times 10^{-26}$ for the 38 low luminosity AGN. The best fit to the correlation (after considering the error in the determination of the luminosity of narrow H$\alpha$) is given by:

$$\log(L_{H\alpha_N}) = (1.373\pm0.032)+(0.915\pm0.003)\times\log L_{5100\mathring{A}} \mathrm{erg \cdot s^{-1}} \quad (9)$$

This result indicates that the effects of the inclination angle can be neglected for the correlation between the spectral index and the dimensionless accretion rate.

The correlation between spectral index and dimensionless accretion rate found in this research provides another independent method to estimate the central BH masses of AGN. The spectral index and continuum luminosity can be directly determined from the observed spectrum in the optical band, and subsequently the Eddington Luminosity, i.e. BH masses, can be determined by means of the correlation we found. This method has the advantage of being independent of the different correlations between the size of the BLRs and the continuum luminosity in Equation (2). Also, this method can be applied when it is not possible to measure the stellar velocity dispersion of the bulge. In future work, we will estimate the BH masses of QSOs with higher redshift using this method to solve the problem of why virial BH masses of QSOs estimated by Equation (2) lead to BH masses larger than $10^{10} M_{\odot}$, while observational results (fortunately) seem to contradict this result (Dultzin-Hacyan et al. 2007).

Finally, a simple summary is as follows. We first select 193 AGN with both broad H$\alpha$ and broad H$\beta$, and with apparent absorption MgI$\lambda$5175$\mathring{A}$ from SDSS DR4. Then after the determination of the spectral index (after the correction of internal reddening effects through the Balmer decrements for broad Balmer emission lines, and after the subtraction of stellar component) and dimensionless accretion rate ($\frac{9\times L_{5100\mathring{A}}}{L_{Edd}}$), we find a strong correlation between these parameters for AGN, which provides another independent and method to estimate the central BH masses of AGN.

## ACKNOWLEDGEMENTS

ZXG gratefully acknowledges the postdoctoral scholarships offered by la Universidad Nacional Autonoma de Mexico (UNAM). D. D. acknowledges support from grant IN100507 from PAPIIT, DGAPA, UNAM. This paper has made use of the data from the SDSS projects. Funding for the creation and the distribution of the SDSS Archive has been provided by the Alfred P. Sloan Foundation, the Participating Institutions, the National Aeronautics and Space Administration, the National Science Foundation, the U.S. Department of Energy, the Japanese Monbukagakusho, and the Max Planck Society. The SDSS is managed by the Astrophysical Research Consortium (ARC) for the Participating Institutions. The Participating Institutions are The University of Chicago, Fermilab, the Institute for Advanced Study, the Japan Participation Group, The Johns Hopkins University, Los Alamos National Laboratory, the Max-Planck-Institute for Astronomy (MPIA), the Max-Planck-Institute for Astrophysics (MPA), New Mexico State University, Princeton University, the United States Naval Observatory, and the University of Washington.

## REFERENCES

Adelman-McCarthy J. K., et al., 2006, ApJS, 162, 38
Antonucci R., 1993, ARA&A, 31, 473
Bonning E. W., Shields G. A., Salviander S., Cheng L., Gebhardt K., 2007, ApJ, 659, 211
Dultzin-Hacyan D., Marziani P., Sulentic J. W., 2007, Black Holes: From Stars to Galaxies - Across the Range of Masses, International Astronomical Union. Symposium no. 238, held 21-25 August, 2006 in Prague, Czech Republic, 238, 13
Ferrarese L., Merritt D., 2000, ApJ, 539, L9
Fitzpatrick E. L., 1999, PASP, 111, 63
Francis P. J., Hewett P. C., Foltz C. B., et al., 1991, ApJ, 373, 465
Gebhardt K., et al., 2000, ApJ, 539, L13
Greene J. E., Ho L. C., 2005a, ApJ, 627, 721
Greene J. E., Ho L. C., 2005b, ApJ, 630, 122
Hao L., et al., 2005, AJ, 129, 1783
Häring, N., Rix, Hans-Walter, 2004, ApJ, 640, L89
Ho L. C., Filippenko A. & Sargent W. L. W., 1997a, ApJS, 112, 315
Ho L. C., Filippenko A. & Sargent W. L. W., 1997b, ApJS, 112, 391
Ho L. C., 1999, ApJ, 516, 672
Kaspi S., Smith P. S., Netzer H., Maoz D., Jannuzi B. T., Giveon U., 2000, ApJ, 533, 631
Kaspi S., Maoz D., Netzer H., Peterson B. M., Vestergaard M., Jannuzi B. T., 2005, ApJ, 629, 61
Kauffmann G., et al., 2003, MNRAS, 346, 1055
Kormendy J., 2001, in Galaxy Disks and Disk Galaxies, proceeding of a conference held in Rome, Italy, June 12-16, 2000 at the Pontifical Gregorian University and sponsored by the Vatican Observatory. ASP Conference Series, Vol. 230. Edited by Jose G. Funes, S. J. and Enrico Maria Corsini. San Francisco: Astronomical Society of the Pacific. ISBN: 1-58381-063-3, 2001, pp. 247-256
Laor A., 2001, ApJ, 533, 677
Le Borgne J. F., et al., 2003, A&A, 402, 433

Li C., Wang T. G., Zhou H. Y., Dong X. B., Chen F. Z., 2005, AJ, 129, 669
Marconi A., Hunt L. K., 2003, ApJ, 589, L21
McLure R. J., Dunlop J. S., 2002, MNRAS, 331, 795
Merritt D., Ferrarese L., 2001, ApJ, 547, 140
Netzer H., 2003, ApJ, 583, L5
Onken C. A., Ferrarese L., Merritt D., Peterson B. M., Pogge R. W., Vestergaard M., Wandel A., 2004, ApJ, 615, 645
Panessa F., Bassani L., Cappi M., Dadina M., Barcons X., Carrera F. J., Ho L. C., Iwasawa K., 2006, A&A, 455, 173
Peterson B. M., et al., 2004, ApJ, 613, 682
Quintilio, R.; Viegas S. M., 1997, ApJ, 474, 616
Rix H.-W., White S. D. M., 1992, MNRAS, 254, 389
Shang Z., Brotherton M. S., Green R. F., Kriss G. A., Scott J., Quijano J. K., 2005, ApJ, 619, 41
Sulentic J. W., Repetto P., Stirpe G. M., Marziani P., Dultzin-Hacyan D., Calvani M., 2006, A&A, 456, 929
Tremaine S., Gebhardt K., Bender R., Bower G., et al., 2002, ApJ, 574, 740
Urry C. M., Padovani P., 1995, PASP, 107, 803
Vanden Berk, D. E., et al., 2001, AJ, 122, 549
Wandel A., 1999, ApJ, 519, L39
Wang T.-G., Zhang X.-G., 2003, MNRAS, 340, 793
Zhang X.-G., Dultzin-Hacyan D., Wang T.-G., 2007a, MNRAS, 374, 691
Zhang X.-G., Dultzin-Hacyan D., Wang T.-G., 2007b, MNRAS, 376, 1335
Zhang X.-G., Dultzin-Hacyan D., Wang T.-G., 2007c, MNRAS, 377, 1215
Zheng W., Kriss G. A., Telfer R. C., Grimes J. P., Davidsen A. F., 1997, ApJ, 475, 469

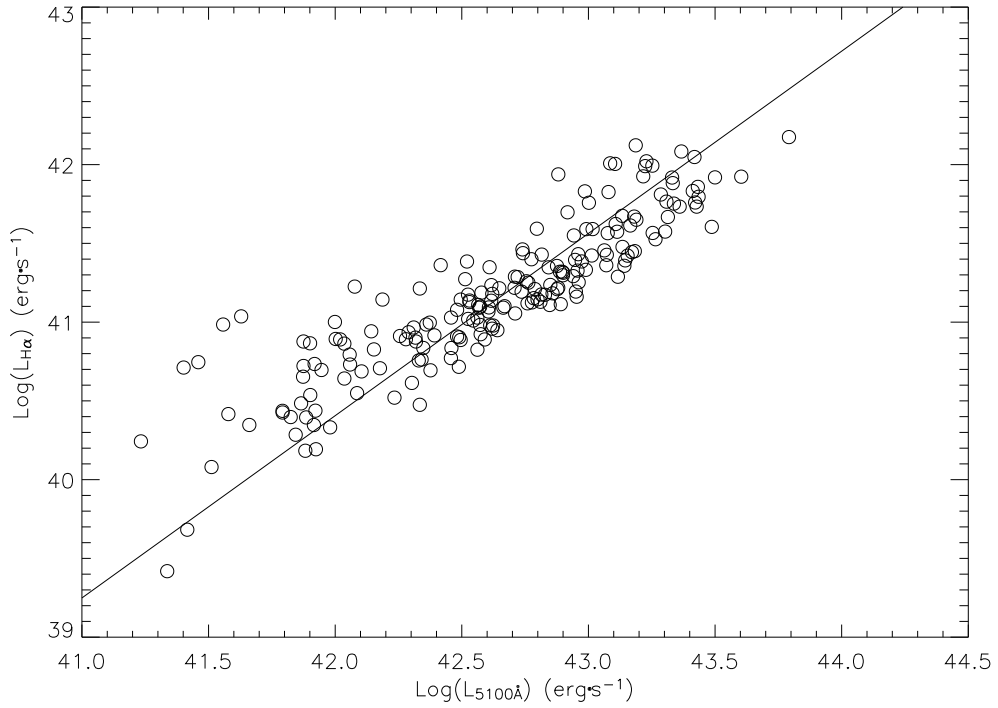


**Figure 1.** The correlation between the continuum luminosity and the luminosity of H$\alpha$ before the internal reddening correction. The solid line represents the correlation found by Greene & Ho (2005b).

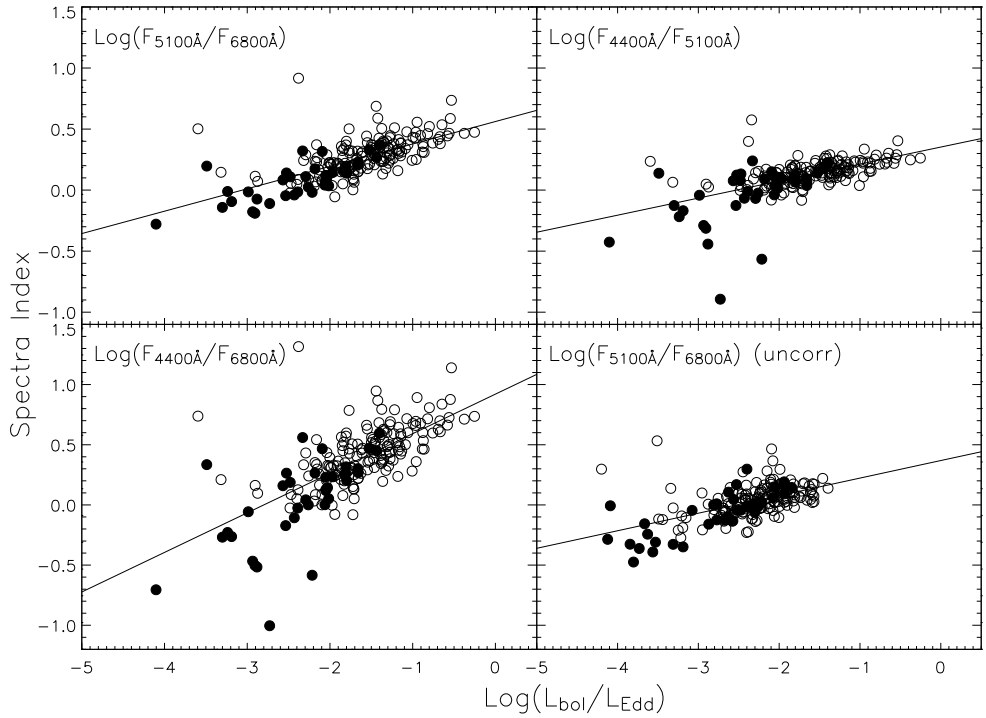


**Figure 2.** The correlation between the spectral index and the dimensionless accretion rate. The solid line represents the unweighted best fitted result. Solid circles represent low luminosity AGN with luminosity of H$\alpha$ less than $10^{41}\mathrm{erg}\cdot\mathrm{s}^{-1}$ as identified in Ho et al. (1997a, 1997b), open circles are normal AGN.

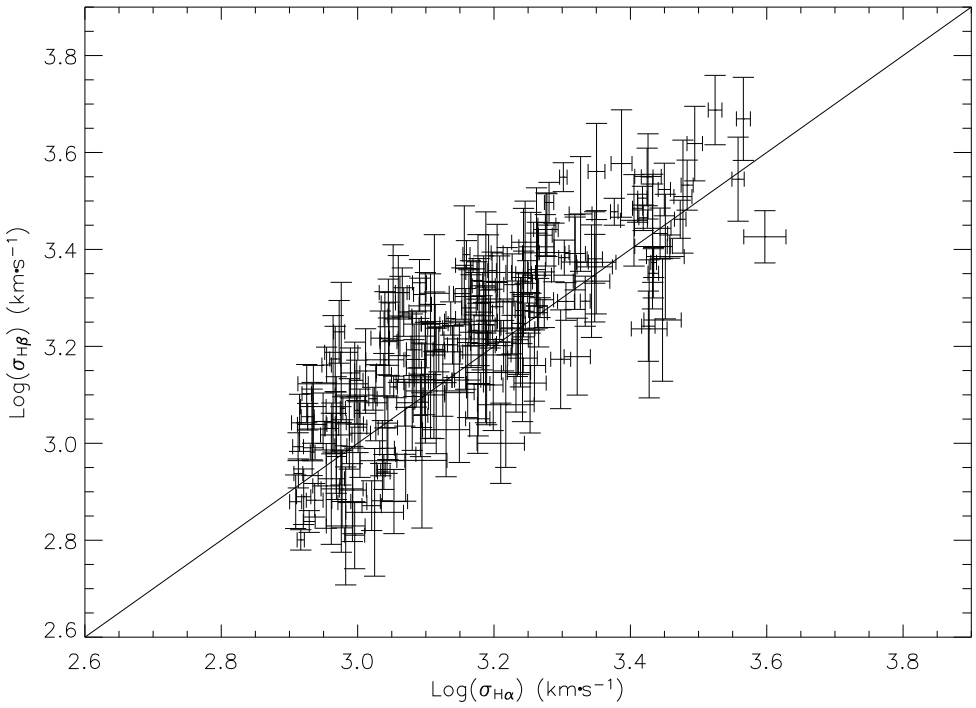


**Figure 3.** The correlation between the line widths of broad H$\alpha$ and broad H$\beta$. The solid line represents the relation: $\sigma_{H\alpha}(B) = \sigma_{H\beta}(B)$.

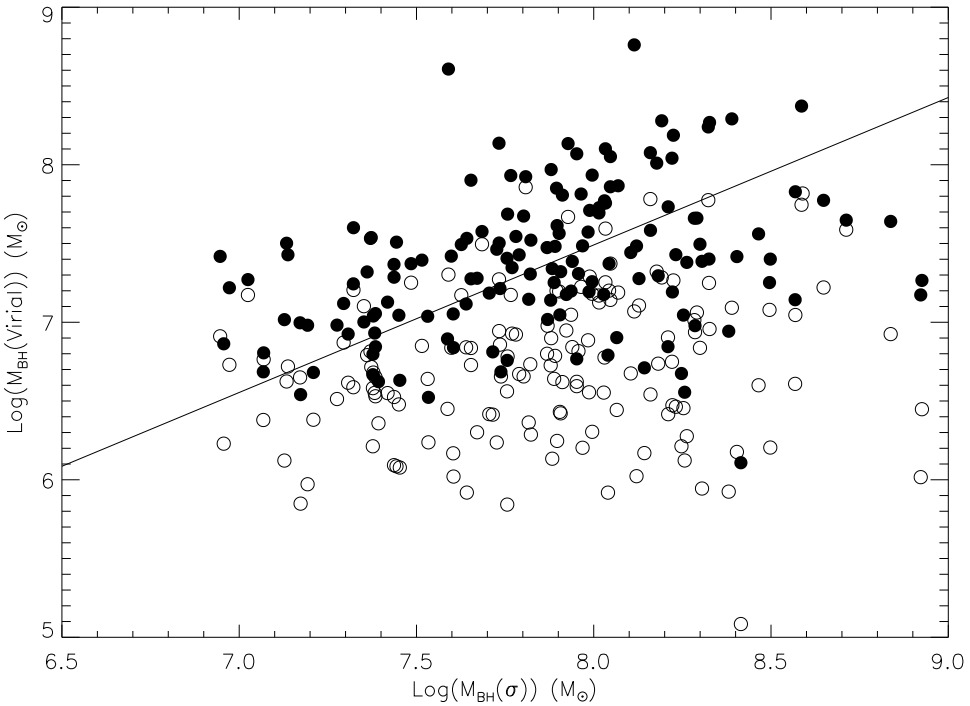


**Figure 4.** The correlation between the two kinds of BH masses, $M_{BH}(\sigma)$ estimated from Equation (1) and $M_{BH}(Virial)$ estimated from Equation (2). The solid line represents the relation: $\log(M_{BH}(\sigma)) = 1.06\log(M_{BH}(Virial))$. Solid circles represent calculations after the internal reddening correction, open circles are the values before the internal reddening correction.

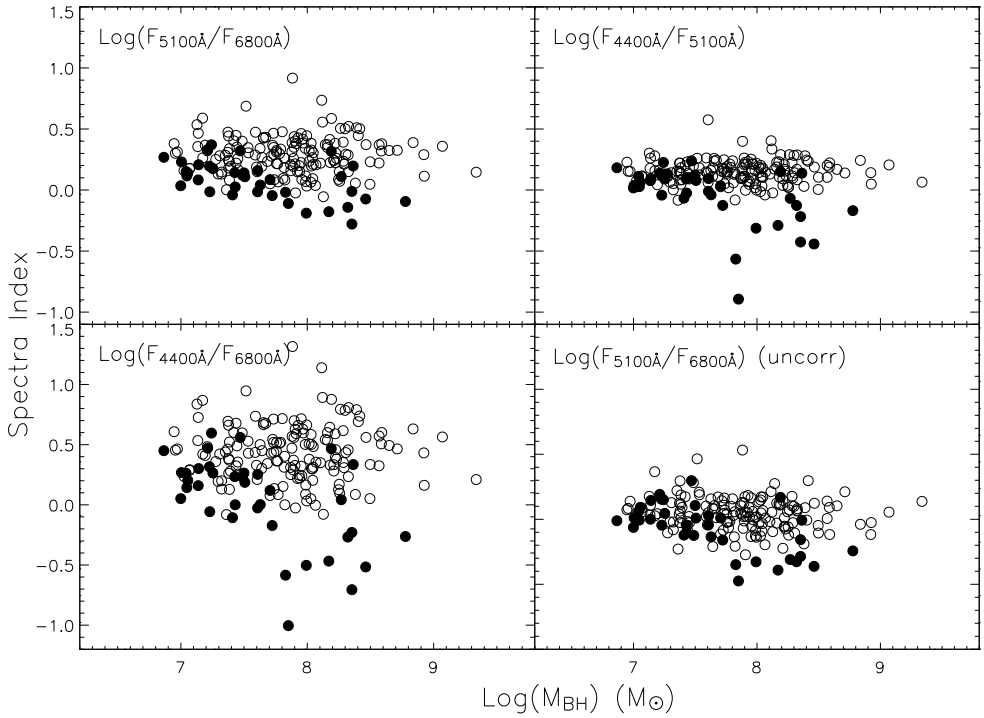


**Figure 5.** The correlation between the spectral index and the central BH mass. Solid circles represent the low luminosity AGN with luminosity of H$\alpha$ less than $10^{41}\mathrm{erg}\cdot\mathrm{s}^{-1}$ as identified in Ho et al. (1997a, 1997b). Open circles are the normal AGN.

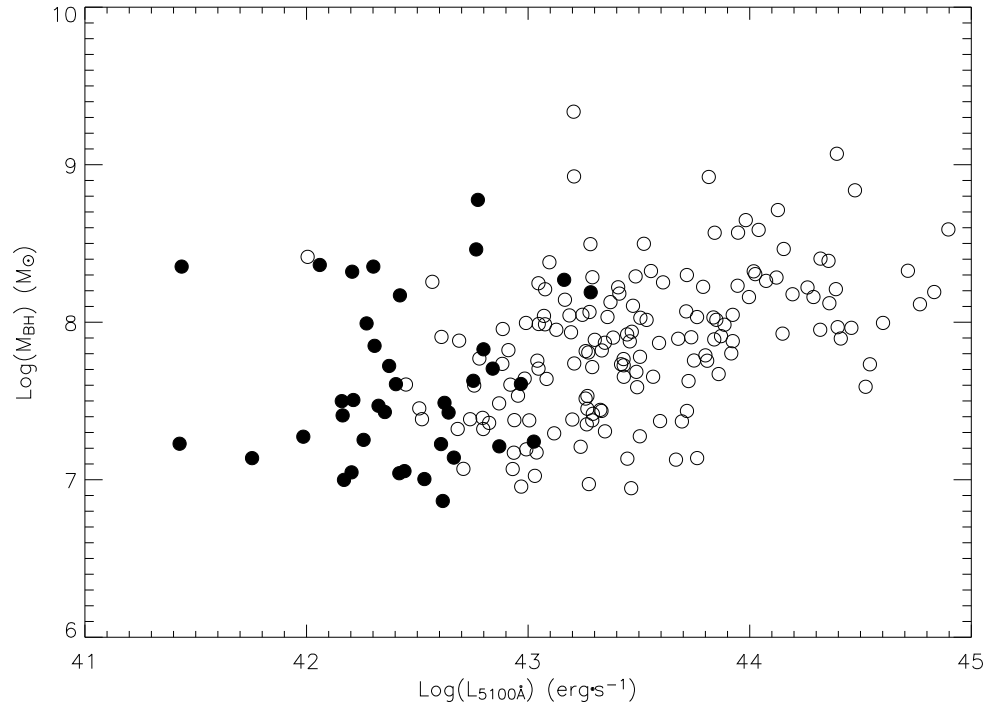


**Figure 6.** The correlation between the central BH mass and the continuum luminosity after the correction of internal reddening effects. Solid circles represent the low luminosity AGN with luminosity of H$\alpha$ less than $10^{41}\mathrm{erg}\cdot\mathrm{s}^{-1}$ as identified in Ho et al. (1997a, 1997b),open circles are the normal AGN.

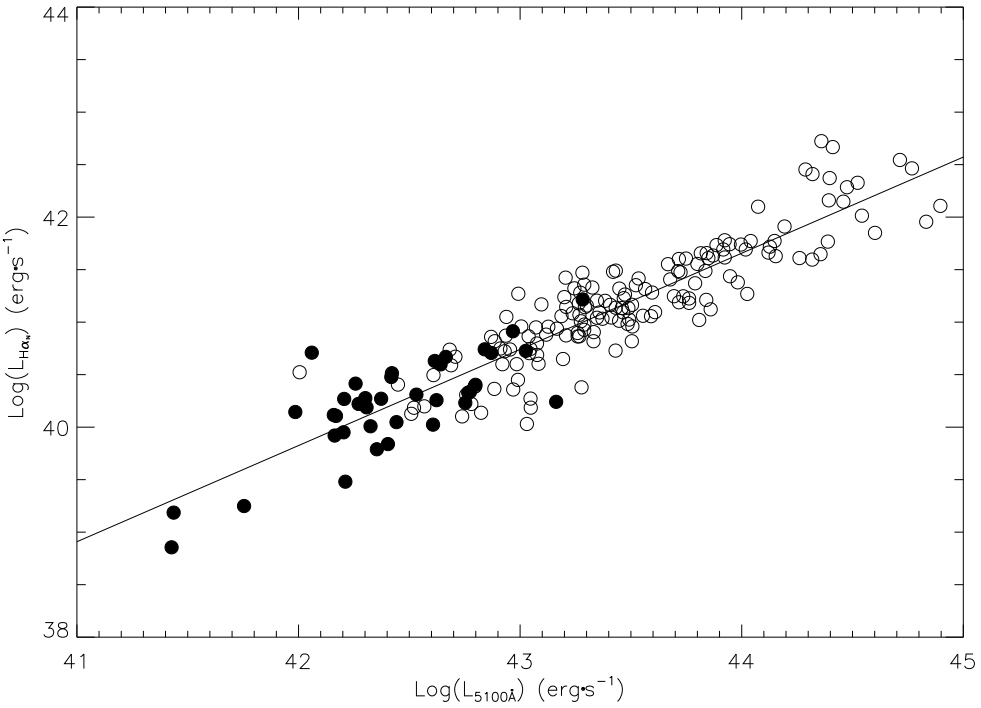


**Figure 7.** The correlation between the continuum luminosity and the luminosity of narrow H$\alpha$ after the correction of internal reddening effects. Solid circles represent the low luminosity AGN with luminosity of H$\alpha$ less than $10^{41}\mathrm{erg}\cdot\mathrm{s}^{-1}$ as identified in Ho et al. (1997a, 1997b), open circles are the normal AGN. The solid line represents the best fit $L_{H\alpha_N} \propto L_{5100\mathring{A}}^{0.915\pm0.003}$.